Rev. Ivoir. Sci. Technol., 43 (2024) 122 - 131
ISSN 1813-3290, http://www.revist.ci

CONOIDAL CRACK WITH ELLIPTIC BASES, WITHIN CUBIC CRYSTALS, UNDER ARBITRARILY APPLIED LOADINGS - II. APPLICATION TO MECHANICAL TWINNING OF [112] COPPER SINGLE CRYSTALS

P. N. B. ANONGBA

Université F.H.B. de Cocody, U.F.R. Sciences des Structures de la Matière et de Technologie, 22 BP 582 Abidjan 22, Côte d'Ivoire

(reçu le 28 Avril 2024; accepté le 11 Juin 2024)

* Correspondance, e-mail : *anongba@gmail.com*

ABSTRACT

In this part II graphical plots of $<\tilde{G}>$ normalized average crack extension force, as a function of (θ_0, ϕ_0) defining crack and twinning systems, have been displayed. Positive $<\tilde{G}>$ are observed indicating that these deformation systems can operate under the specified conditions. Configurations of local $<\tilde{G}>$ maximum are identified suggesting these correspond to equilibrium states. A minimum size is required for the growing of the nucleus of a given deformation system; this can be determined. A connection between subboundaries of pure tilt character, perpendicular to primary octahedral {111} slip planes, and twinning systems is stressed.

Keywords : *fracture mechanics, linear elasticity, dislocations, crack extension force, high temperature mechanical twinning.*

RÉSUMÉ

Fissure conoïdale à base elliptique dans un cristal cubique sous sollicitations extérieures arbitraires – II. Application au maclage mécanique de monocristaux de cuivre d'axe [112]

Dans cette partie II, des tracés graphiques de $<\tilde{G}>$ force d'extension moyenne normalisée de fissure, en fonction de (θ_0, ϕ_0) définissant les systèmes de fissure et macle, sont affichés. Des $<\tilde{G}>$ positifs sont observés indiquant que ces systèmes de déformation peuvent fonctionner dans les conditions spécifiées. Des configurations de maximum local $<\tilde{G}>$ sont identifiées, suggérant qu'elles

correspondent à des états d'équilibre. Une taille minimale est requise pour la croissance du germe d'un système de déformation donné ; cela peut être déterminé. Une connexion entre des sous joints de flexion pure, perpendiculaires aux plans de glissement octaédriques primaires {111}, et des systèmes de maclage est soulignée.

Mots-clés : *mécanique de la rupture, élasticité linéaire, dislocation, force d'extension de fissure, maclage mécanique à haute temperature.*

I - INTRODUCTION

In the first part of this study [1], we have considered a conoidal nucleus of crack (vertex O) within an infinitely extended cubic material, arbitrarily oriented (O; x_j') with respect to the laboratory reference frame (O; x_j); the latter indicates the directions x_j of the externally applied loads ***(Figure 1)***. The general loading corresponds to tension σ_{22}^a and shears σ_{21}^a and σ_{23}^a along x_2, x_1 and x_3, respectively. The nucleus has been represented by a continuous distribution of infinitesimal elliptic dislocation loops. The problem then addressed is to find the conditions for its growing in steady motion (equilibrium dislocation distributions, boundary front stresses and extension force G per unit length) [1]. Earliest works on the same lines have been :

- The problem of finding the equilibrium form of a linear array of straight dislocations [2 - 4]
- Elastic properties of pair of dislocation walls, with opposite Burgers vectors, perpendicular to dislocation slip planes [5]
- Description of a crack under mode I loading by a continuous distribution of freely climbing edge dislocations ([6], see also [4]).

Because the boundary of a twinned region inside a material can be filled by partial dislocations, all these predecessors [2 - 6] recognized that the growing of a twin nucleus can be studied on the equal manner; this is stressed in different figures (see Fig. 6.35 and Fig.10.11 in [6]). Coming back to ***Figure 1*** and *part I* of this study [1], induced normal Poisson's stresses $-\nu_A(j)\sigma_{22}^a$ along x_1 (j=1) and x_3 (j=3) are considered. $O\,x_2'$ is a symmetrical axis of the crack nuclei. In $x_1'x_3'-$planes the bases are elliptical, with semiaxes ρ_1 and ρ_2 along x_1' and x_3', such that $a_r = \rho_1 / \rho_2$ = constant about any elevation $x_2' = OO' \equiv h$ along $O\,x_2'$. The running position P_D (x_1', x_2', x_3') at the elevation h along the base is written with respect to (O; x_j') as

$$\overrightarrow{OP}_D = \begin{pmatrix} x_1' = \rho \sin\phi \\ x_2' = h = \rho_1 \tan\theta \\ x_3' = \rho\cos\phi \end{pmatrix} ; \ -\pi \le \phi \le \pi , \quad 0 \le \theta < \pi/2;$$

$$\rho^2 = \rho_1^2 / (\sin^2\phi + a_r^2 \cos^2\phi) . \qquad (1)$$

The angle ϕ is between $O'x_3'$ and $O'P_D$ as shown in ***Figure 1***. Angle θ is measured in $Ox_1'x_2'$ between $\boldsymbol{P_D}$ ($\phi = \pi/2$) $\boldsymbol{O'}$ and $\boldsymbol{P_D}$ ($\phi = \pi/2$) $\boldsymbol{O}$ where P_D ($\phi = \pi/2$) has elevation $x_2' = h$ from $Ox_1'x_3'$; its alternate interior angle is shown in ***Figure 1***. Additional angular parameters θ_0 and ϕ_0 (Euler's angles) are introduced that connect $\vec{x}_j$ to $\vec{x}_j'$.

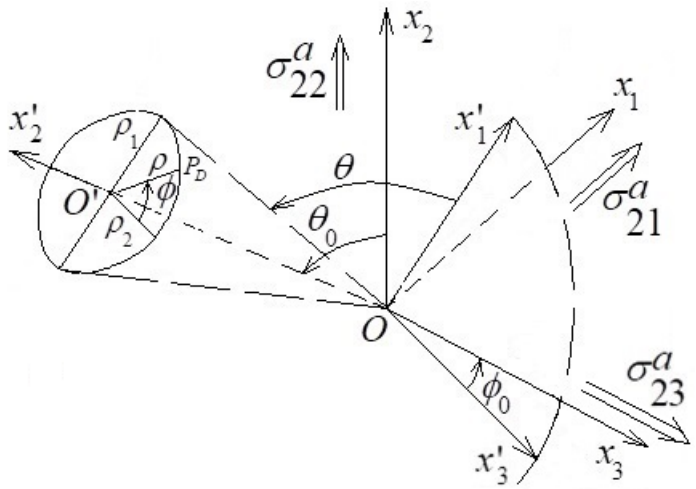

Figure 1 : *Elliptical base (elevation $x_2' = OO' \equiv h$) of the conoidal crack with semiaxes ρ_1 and ρ_2 along x_1' and x_3'. The running point P_D (1) along the base and angular parameters θ_0 and ϕ_0 that connect $\mathbf{x}_j$ and $\vec{x}_j'$ are illustrated. Angle θ is introduced by the relation* $\tan\theta = OO'/\rho_1$. *The medium suffers uniformly applied tension σ_{22}^a in the vertical x_2 - direction and shears σ_{21}^a and σ_{23}^a (parallel to the horizontal x_1x_3- plane) in the x_1 and x_3 directions*

In this *part II*, the treatment in [1] with associated model illustrated in ***Figure 1*** is applied to the abundant mechanical twinning observed in [112] copper single crystals deformed at constant strain rates and elevated temperatures (773 to 1173 *K*) [7 – 11]. In *Section* 2, experimental findings (mechanical behaviour

and microstructure) connected to twinning are summarized and the methodology of the treatment is given. In *Section* 3, graphical representations of < *G* > (see relation (34) in [1]), *G* averaged over the whole twin expanding front, are displayed corresponding to different twinning systems; these results are discussed. *Section* 4 is devoted to conclusion.

II - METHODOLOGY

[112] copper single crystals have been deformed vertically (x_2 = [112], ***Figure 1***) under constant strain rate tests $\dot{\varepsilon} = m\dot{\gamma}$. The resolved shear stresses τ ($\sigma_{22}^{a} = \tau / m$) and strain γ have been calculated with Schmid factor m = 0.41 of the two primary octahedral slip systems [101]($\bar{1}11$) and [011]($1\bar{1}1$). A stereographic projection with centre [112] is provided for illustration and identification, ***Figure 2***.

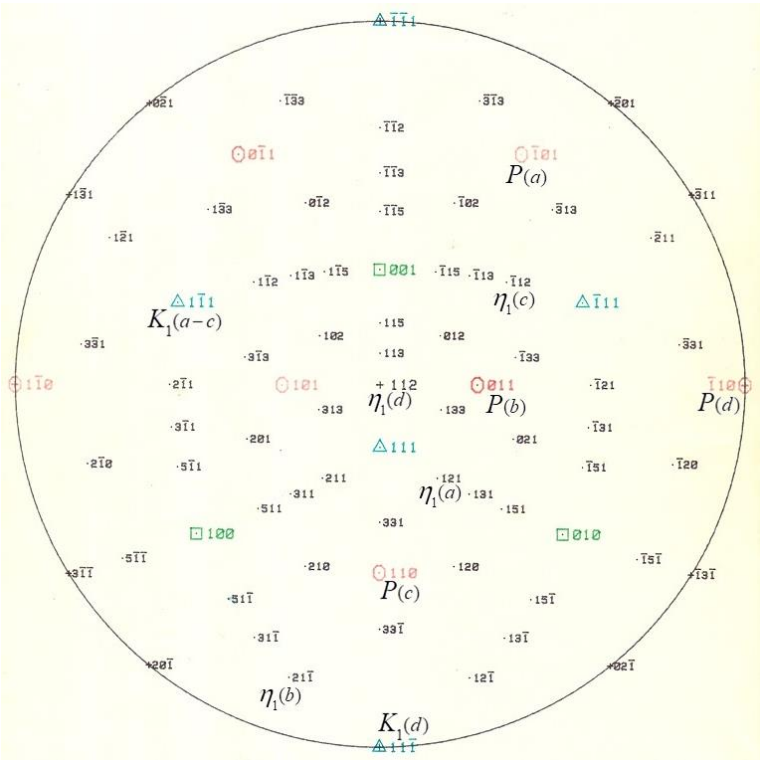

Figure 2 : *Stereographic projection with centre* [112] *for the identification of slip and twinning systems in* [112] *copper single crystals deformed between 773 and 1173 K at constant strain rates*

In temperature regime 2 (773 – 1173 *K*, approximately), the deformation begins with the motion of perfect ½ <011> dislocations. At a well-defined shear stress level denoted τ_V, abundant mechanical twinning set in at different places in the sample. This deformation mode defined what has been named stage V. Twins occupy volumes of the order of 1 mm^3 late in this stage (see Figs. 86 and 87 in [7]). Identified twinning planes are $(\bar{1}11)$ and $(1\bar{1}1)$ with associated imperfect 1/6 <121> dislocations [7]. The designation of a twinning system is given in ***Figure 3***.

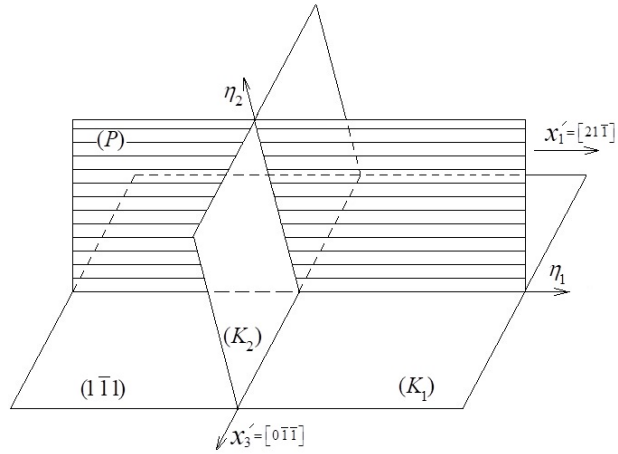

Figure 3 : *Designation of a twinning system TS and dislocation wall perpendicular to octahedral slip plane. The twinning and conjugate (or reciprocal) planes are (K_1) and (K_2), respectively; the twinning and conjugate (or reciprocal) directions are η_1 and η_2, respectively. η_1, η_2 and the normals to (K_1) and (K_2) are all contained in the plane of shear (P). The dislocations are all parallel to $x_1' = [21\bar{1}]$, form a plane (P) = $(0\bar{1}\bar{1})$, with different Burgers vectors ½[011], ½[110] and ½ $[10\bar{1}]$ in the primary slip plane $(1\bar{1}1)$*

For the application (*Section* 3), we shall consider the following twinning systems *TS(i), i= a, b, c, d* with corresponding twinning elements (the x_j in ***Figure 1*** are unchanged):

(1) *TS(a)*: $K_1(a) = (1\bar{1}1)$, $\eta_1(a) = [121]$, $K_2(a) = (111)$, $\eta_2(a) = [\bar{1}2\bar{1}]$, $P(a) = (10\bar{1})$; using ***Figure* 1** and indicating the direction only, we have $x_2' = [1\bar{1}1]$, $x_1' = \eta_1(a)$, $x_3' = x_1' x_2' = [10\bar{1}]$; $\vec{x}_1 = \left[\bar{2}4\bar{1}\right]$, $\vec{x}_2 = [112]$, $\vec{x}_3 = \left[31\bar{2}\right]$, $\theta_0 = 62°$, $\phi_0 = 19°$;

(2) *TS(b)*: $K_1(b) = (1\bar{1}1)$, $\eta_1(b) = [21\bar{1}]$, $K_2(b) = (11\bar{1})$, $\eta_2(b) = [2\bar{1}1]$, $P(b) = (0\bar{1}\bar{1})$; $x_2' = [1\bar{1}1]$, $x_1' = \eta_1(b)$, $x_3' = [0\bar{1}\bar{1}]$; $\theta_0 = 62°$, $\phi_0 = 80°$;

(3) *TS(c)*: $K_1(c) = (1\bar{1}1)$, $\eta_1(c) = [1\bar{1}2]$, $K_2(c) = (\bar{1}11)$, $\eta_2(c) = [1\bar{1}2]$, $P(c) = (\bar{1}\bar{1}0)$; $x_2' = [1\bar{1}1]$, $x_1' = \eta_1(c)$, $x_3' = [\bar{1}\bar{1}0]$; $\theta_0 = 62°$, $\phi_0 = 140°$;

(4) *TS(d)*: $K_1(d) = (11\bar{1})$, $\eta_1(d) = [112]$, $K_2(d) = (111)$, $\eta_2(d) = [11\bar{2}]$, $P(d) = (\bar{1}10)$; $x_2' = [11\bar{1}]$, $x_1' = \eta_1(d)$, $x_3' = [\bar{1}10]$; $\theta_0 = 90°$, $\phi_0 = 0$.

(2)

The resolved shear stress τ_V at the beginning of twinning stage V has been found thermally activated, satisfying an Arrhenius law temperature T dependence [8], in the form:

$$\dot{\gamma} = A(\tau_V - \tau_\mu)^n \exp -\frac{\Delta H}{kT} \quad \text{or}$$

$$\dot{\varepsilon} = m^{n+1} A(\sigma_{22}^a - \sigma_{22}^{fr})^n \exp -\frac{\Delta H}{kT}. \qquad (3)$$

The different quantities $\dot{\gamma}$, τ_V, τ_μ, ΔH and constants A, n, and k are given in [8]. For the present, σ_{22}^a corresponds to τ_V and the friction stress σ_{22}^{fr} to τ_μ (see relation (35) in [1] for the use of (σ_{22}^a - σ_{22}^{fr}) that is called the effective stress). In deformation stage IV that preceded stage V (twinning), the deformation structure consists of subboundaries. These have been described in detail [7, 9 – 11]. We focus on those perpendicular to primary slip planes $(1\bar{1}1)$ and $(\bar{1}11)$ because some geometries recall the twinning geometry in ***Figure 3***. Subboundary planes are close to {011} perpendicular to their dislocation glide planes {111}; they consist of one, two or three dislocation families, all having their Burgers vectors in the same plane and are parallel to the same direction (<112> have been observed below). They are of pure tilt character because the misorientation axis is parallel to the dislocation direction. These dislocation walls are frequently seen in pairs small distances apart (see subboundaries encircling subgrains C_3 and C_1 in Fig. 7 of [10] and Fig. 6 in [11]). A sketch of subboundary *S* of Fig.6 in [11] is depicted in ***Figure 3*** : it consists of families 1, 2, and 3 with $\vec{b}_1 = 1/2[011]$, $\vec{b}_2 = 1/2[110]$ and $\vec{b}_3 = 1/2[10\bar{1}]$, respectively. Family 1 is in equal proportion to both families 2 and 3. Their directions are parallel to $[21\bar{1}] = x_1'$ and their common glide plane is $(1\bar{1}1) = (K_1)$. The normal to the subboundary is $[0\bar{1}\bar{1}] = x_3'$. The misorientation angle is 0.6°. We next consider <*G*> obtained in the first part of this study (see relation (34) of [1]) and present below graphical plots of its normalized value $< \tilde{G} >$ defined as

$$< \tilde{G} >=< G > /G_C^I =< \tilde{G} > (\theta, \theta_0, \phi_0, M_{12}, M_{13}, a_r, C_{nm}),$$

$$G_C^I = \frac{2^5 \alpha_0^2 a_r^4}{3\pi^2 C_{44}} (K_I^0)^2; \quad (4)$$

where $K_I^0 = \sigma_{22}^a \sqrt{\pi a_1}$, $M_{12} = \sigma_{21}^a / \sigma_{22}^a$ and $M_{13} = \sigma_{23}^a / \sigma_{22}^a$. The applied stresses are viewed as effective stresses acting on the dislocations in the medium. The room temperature average values C_{11}= 1.691, C_{12}= 1.222 and C_{44} = 0.7542 in units of [$10^{11} N / m^2$] for copper have been used (see *Table* 2 in [12]).

III - RESULTS AND DISCUSSION

We focus on the twinning system *TS(a)* (2) and plot $< \tilde{G} >$ as a function of θ, ***Figure 4***.

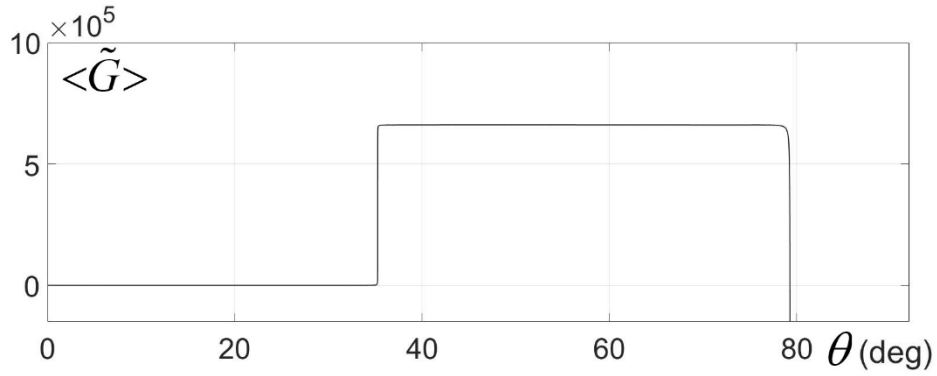

Figure 4 : $< \tilde{G} >$ *(4) as a function of* θ *for the twinning system TS(a) (2);* $M_{12} = M_{13} = 10^{-4}$, $\nu_A(1) = \nu_A(3) = 1/3$, a_r = *4 / 3*

$< \tilde{G} >$ is negative or nearly zero in θ interval [0, 35°] and clearly negative in [79°, 90°] approximately; it becomes clearly positive between [35°, 79°], approximately. Negative and positive values indicate forbidden and possible evolution of the system, respectively. ***Figure 5*** is a plot of $< \tilde{G} >$ as a function of ϕ_0 for $\theta = \pi / 3$ and θ_0 = 62°.

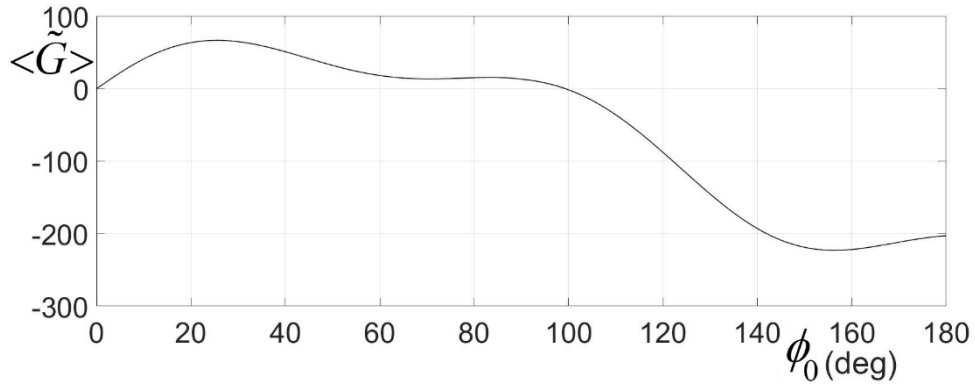

Figure 5 : $<\tilde{G}>$ *(4) as a function of* ϕ_0 *for* $\theta = \pi/3$ *and* $\theta_0 = 62°$*. This corresponds to identical twinning plane* $(1\bar{1}1)$ *and the twinning systems TS(a)* ($\phi_0 = 19°$)*, TS(b)* ($\phi_0 = 80°$) *and TS(c)* ($\phi_0 = 140°$)*.* $M_{12} = M_{13} = 10^{-4}$, $\nu_A(1) = \nu_A(3) = 1/3$, $a_r = 4/3$

This concerns the identical twinning plane $(1\bar{1}1)$: ϕ_0 = 19°, 80° and 140° for the twinning systems *TS(a)*, *TS(b)* and *TS(c)*, respectively. These have positive $<\tilde{G}>$ for *TS(a)* and *TS(b)* indicating that their evolutions are feasible. *TS(c)* displays negative values suggesting that it is forbidden. *TS(b)* is close to $\partial <\tilde{G}> / \partial \phi_0 = 0$ (local average $<\tilde{G}>$ maximum) as well as *TS(a)* taking account of available twinning system around. ***Figure 6*** shows $<\tilde{G}>$ as a function of θ_0 for $\theta = \pi/2$ and $\phi_0 = 0$.

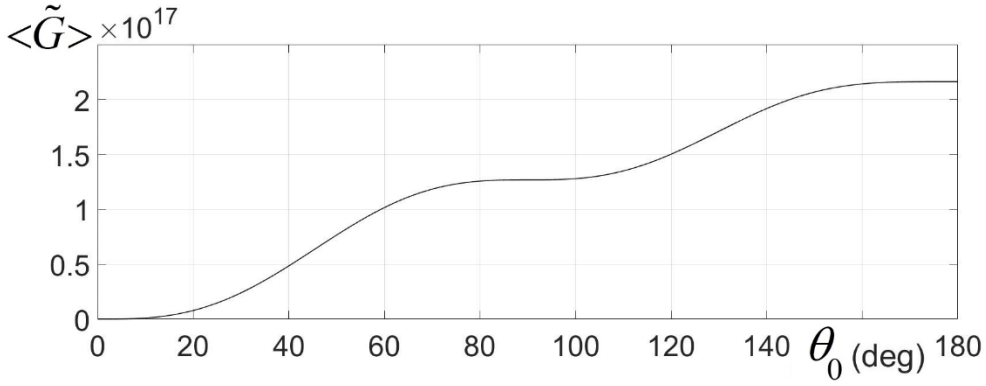

Figure 6 : $<\tilde{G}>$ *(4) as a function of* θ_0 *for* $\theta = \pi/2$ *and* $\phi_0 = 0$*. For* $\theta_0 = 90°$*, this corresponds to the twinning system TS(d) of the deviation plane* $(11\bar{1})$*. A local maximum is observed.* $M_{12} = M_{13} = 10^{-4}$, $\nu_A(1) = \nu_A(3) = 1/3$, $a_r = 4/3$

Figure 3 shows a correspondence of configurations between a dislocation wall $(0\bar{1}\bar{1})$ perpendicular to primary octahedral slip plane $(1\bar{1}1)$ and a twinning system *TS(b)* (*Section* 3). The dislocation wall consists of perfect ½< 110 > dislocations with direction $[21\bar{1}]$. To *TS(b)* is associated arrays of parallel imperfects 1/6< 112 > in plane (*P*). Both types of wall satisfy the Frank criterion (see [13]) for dislocation arrangements in equilibrium as common property. A pair of subboundary *S* (Fig. 6 in [11]) with opposite Burgers vectors may well be a nucleus of *TS(b)* by the motion in $(1\bar{1}1)$ of partial dislocations $1/6[21\bar{1}]$. In pursuing, we first focus on ***Figure 4***. From θ = 0 to 35°, $<\tilde{G}>$ is nearly zero or negative indicating that the growing of nuclei of twinning is rejected under such conditions. Hence to be able to grow, a minimum height $OO'_{\min} = \rho_1 \tan[35\pi/180]$ for the nuclei is required. In the case of cracks, the fractography of the surfaces of broken specimens in high-cycle fatigue experiments [14 – 16] reveals the presence of defects (inclusions, heterogeneities, cavities …) at the vertex *O* of observed conoidal cracks. The sizes of these defects may give experimental values for ρ_1 and $OO'_{\min}$. We now consider ***Figure 5***. In the situation of cracks, stationary configurations correspond to ϕ_0 = 22° and 72°, approximately. These are the configurations that sustain large deformations over time. In the situation of twinning along a <112> direction, both *TS(a)* and *TS(b)* system are stationary. *TS(c)* is forbidden. The plane of deviation $(11\bar{1})$ is also of interest ***(Figure 6)***. Indeed *TS(d)* (ϕ_0= 0, θ_0 = 90°) is stationary. It has been checked that for $\theta = \pi/3$, the magnitudes of $<\tilde{G}>$ observed for *TS(a)*, *TS(b)* and *TS(d)* are similar. Configurations of average $< G >$ maximum are revealed by the quantity $<\tilde{G}>$ (4). G_C^I (4) contains K_I^0 (commonly named stress intensity factor) and carries the Arrhenius law temperature *T* dependence linking the effective applied stress and the strain rate (3).

IV - CONCLUSION

This study concerns [112] copper single crystals deformed at constant strain rates between 773 and 1173*K* (temperature regime 2 [7 - 11]). Graphical plots of $<\tilde{G}>$ (4) as a function of (θ_0, ϕ_0) defining crack and twinning systems, have been displayed. Positive $<\tilde{G}>$ are observed indicating that these deformation systems can operate under the specified conditions. Configurations of local $<\tilde{G}>$ maximum are identified suggesting these correspond to equilibrium states. A minimum size is required for the growing of the nucleus of a given deformation system; this can be determined. A connection between subboundaries of pure tilt character, perpendicular to primary octahedral {111} slip planes and twinning systems has been stressed.

REFERENCES

[1] - P. N. B. ANONGBA, Conoidal crack with elliptic bases, within cubic crystals, under arbitrarily applied loadings – I. Dislocations, crack-tip stress and crack extension force, (a) *Rev. Ivoir. Sci. Technol.*, 43 (2024) In press (b) *ResearchGate*, DOI: 10.13140/RG.2.2.21165.67044

[2] - J. D. ESHELBY, F. C. FRANK and F. R. N. NABARRO, The equilibrium of linear arrays of dislocations, *Phil. Mag.*, 42 (1951) 351 - 364

[3] - G. LEIBFRIED, Verteilung von versetzungen im statischen gleichgewicht, *Zeitschrift für Physik*, 130 (1951) 214 - 226

[4] - B. A. BILBY and J. D. ESHELBY, Dislocations and the theory of fracture, In: "Fracture", Ed. Academic Press (H. Liebowitz), New York, Vol. 1, (1968) 99 - 182

[5] - F. C. FRANK and A. N. STROH, On the theory of kinking, *Proc. Phys. Soc., B* 65 (1952) 811 - 821

[6] - J. FRIEDEL, "Dislocations", Pergamon Press, Paris, (1964)

[7] - P. N. B. ANONGBA, Doctorate thesis No. 826, EPFL, Lausanne, (1989)

[8] - P. N. B. ANONGBA, J. BONNEVILLE and J.-L. MARTIN, Hardening stages of [112] copper single crystals at intermediate and high temperature-I. Mechanical behaviour, *Acta metal. Mater.*, 41 (1993) 2897 - 2906

[9] - P. N. B. ANONGBA, J. BONNEVILLE and J.-L. MARTIN, Hardening stages of [112] copper single crystals at intermediate and high temperature-II. Slip systems and microstructures, *Acta metal. Mater.*, 41 (1993) 2907 - 2922

[10] - P. N. B. ANONGBA and J.-L. MARTIN, Dislocation clustering and hardening of copper, Proceedings of the 9th International Conference of the Strength of Materials (ICSMA – 9), Vol. 1, Haifa, Israel, (1991) 203 - 210

[11] - P. N. B. ANONGBA, Subboundary structures in stage IV in [112] copper single crystals deformed at high temperatures, Proceedings of the 7th JIM International Symposium (JIMIS – 7) on Aspects of High Temperature Deformation and Fracture in Crystalline Materials, Nagoya, Japan, (1993) 11 - 18

[12] - H. M. LEDBETTER and E. R. NAIMON, Elastic properties of metals and alloys. II. Copper, *J. Phys. Chem. Ref. Data*, Vol.3, No.4, (1974) 897 - 935

[13] - J. P. HIRTH and J. LOTHE, "Theory of Dislocations", John Wiley, New York, (1982)

[14] - T. SAKAI, Y. SATO and N. OGUMA, Characteristic S-N properties of high-carbon-chromium-bearing steel under axial loading in long-life fatigue, *Fatigue Fract Engng Mater Struct*, 25 (2002) 765 - 773

[15] - H. ABDESSELAM et al., On the crystallographic, stage I like, character of fine granular area formation internal fish-eye fatigue cracks, *Int J Fatigue*, 106 (2018) 132 - 142

[16] - J. C. STINVILLE et al., Fatigue deformation in a polycrystalline nickel base superalloy at intermediate and high temperature : competing failure modes, *Acta Materialia*, 152 (2018) 16 - 33